Langmuir

Article

pubs.acs.org/Langmuir

Photolysis of Phenylalanine in the Presence of Oxidized Carbon Nanotubes

Eduardo Humeres,*[,†] Eduardo Pinheiro de Souza,[†] Nito Angelo Debacher,[†] Regina de F.P.M. Moreira,[‡] Cristiane Nunes Lopes,[‡] Mª Isabel Fernández,[§] J. Arturo Santaballa,[§] Moisés L. Canle,[§] Wido H. Schreiner,[∥] and Abil E. Aliev[⊥]

[†]Departamento de Química and [‡] Departamento de Engenharia Química e Engenharia de Alimentos, Universidade Federal de Santa Catarina, 88040-670 Florianópolis, Santa Catarina Brazil

[§]Group of Chemical Reactivity & Photoreactivity, Department of Physical Chemistry and Chemical Engineering I, Faculty of Sciences, University of A Coruña, E-15071 A Coruña, Spain

[∥]Departamento de Física, Universidade Federal do Paraná, 81531-980 Curitiba, Paraná Brazil

[⊥]Department of Chemistry, University College London, 20 Gordon Street, London WC1H OAJ, United Kingdom

ABSTRACT: Photolyses at 254 nm of phenylalanine (Phe) in aqueous solutions, were carried out in the presence of oxidized carbon nanotubes modified by the reaction with SO_2 (mNTO). Kinetics of the photolyses were followed by UV spectrophotometry at 220 nm, and the products were characterized by HPLC, XPS, and ^{13}C-SSNMR. The ratio of the initial rates of photolysis in the presence and absence of mNTO, k^*/k_o^*, showed a systematic decrease. The photolytic decay of Phe occurs with minor formation of tyrosine. The mass of nanotubes produced an exponential attenuation of the photolytic decomposition of Phe. Total carbon analyses (TCA) showed no inorganic carbon formation after the photolyses. The first-order rate constant of photofunctionalization of mNTO by the insertion of phenylalanine onto the nanotube matrix was calculated from TCA to be k_{in} = 30.1 min^{-1}. Comparison of the XPS spectra of the mNTO before and after the photolysis, using the atom inventory technique, suggests the insertion of Phe along with the extrusion of a sulfide radical anion ($^{\bullet}S^{-}$) which undergo subsequent oxidation to SO_4^{2-}. The obtained results show the effects of mNTO on the photolysis of Phe and provide a new method of photofunctionalization of carbon materials, modified by the intermediates of the reduction of SO_2, with an organic moiety.

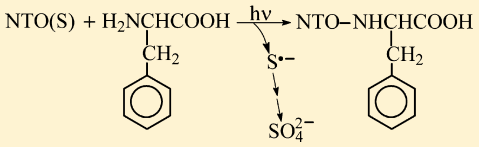

1. INTRODUCTION

Carbon structures and nanostructures present some exceptional physical and chemical properties that are somewhat hampered by their chemical inertness and poor dispersibility. Surface functionalization is important for resolving these problems, as surface-bound functional groups can enhance the surface reactivity of carbon nanostructures as well as the wettability, improving the degree of interfacial binding of the carbon matrix within composite materials.

Modification of carbon nanostructure surfaces is commonly achieved by covalent functionalization and noncovalent wrapping of carbon nanostructures with surfactants, polymers, or ceramic coatings.[1−3]

Carbon nanotubes (NT) are almost exclusively composed of sp^2-bonded carbon atoms, and can be classified as single- and multiwalled carbon nanotubes (SWNT and MWNT).[4] The conductivity of NT is very much dependent on their structural characteristics.[5] SWNT are formed by wrapping a single sheet of graphene, their conductivity depends on their chirality (helicity) and diameter, and may lead to behave as semiconductors or as 1D nanowires. MWNT are composed of coaxial NT cylinders with different chiralities and typical spacing between adjacent layers, close to the interlayer spacing in graphite.[6] They have high electrical conductivity, close to that of graphite at high temperatures and 2D-quantum features at low temperatures.[7]

Nanoparticle-protein conjugates have important applications in clinical chemistry, and functionalized NT can be explored as multipurpose carriers for drug delivery, control of enzymatic activity and diagnostic applications, offering new options in the treatment of complex diseases.[8] Studies on the binding of amino acids, proteins, peptides and enzymes to solid nanoparticles are important because the binding induces changes on the orientation and structure, and consequently, on the reactivity of the different molecules and, in particular, on enzymatic activity.

Carbon nanotubes show a differencial chemical reactivity at the tips and sidewalls.[9] Most reactions are expected to occur at the tips first and then, in some cases, at the sidewalls, especially in the areas where defects are present. This difference in reactivity has led to look for a selective oxidation of the tips, with little structural modification on the sidewalls, using strong oxidant agents[10] that produce hedges functionalized with carboxylic groups.[11]

Received: September 15, 2014
Revised: November 27, 2014
Published: December 11, 2014

DOI: 10.1021/la503631b
Langmuir 2015, 31, 164−170

The reduction of SO_2 on carbon follows the same stoichiometry for a number of different matrices, and the reactivity increases sharply by oxidation and decreasing size and crystallinity of the carbon matrix.[12,13] During the reaction sulfur is rapidly incorporated into the carbon matrix and the XPS spectra in the S 2p region show a band at 163.9 eV (nonoxidized sulfur) and another band at 168.2 eV(oxidized sulfur).[10] A theoretical study of the chemisorption process of SO_2 on the graphite surface using as the active site model a pyrene structure and two dehydrogenated derivatives, showed that at 900 °C the sites of the zigzag edges are completely occupied with a six-membered ring 1,3,2-dioxathiolane **1** and a five-membered ring 1,2-oxathiolane 2-oxide or γ-sultine **2** (Figure 1).[14] Both species of oxidized sulfur intermediates, **1** and **2**, are in equilibrium. Figure 1 shows the postulated primary mechanism involved in the SO_2 reduction on carbons where the zigzag diradical fragment represents the active site of the carbon matrix.[15] The oxidized intermediate **1** decomposes to produce a nonoxidized sulfur intermediate episulfide **3** that initiates a transport mechanism of sulfur out the carbon matrix.[15] The sulfur transfer from the dioxathiolane to produce the reduced episulfide must generate an oxidized moiety $C(CO_2)$ that produces CO_2 in a later step. This mechanism has been found consistent for different types of carbons, such as charcoal, graphite, graphite oxide, graphene oxide and activated carbon.[12,13,15,16]

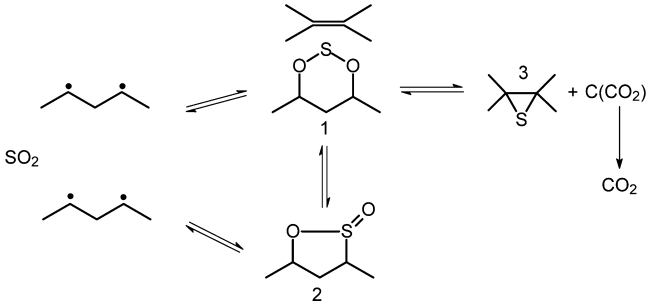

Figure 1. Mechanism of the primary reaction for SO_2 reduction on carbons.

The reactivity of the intermediates of the reduction of SO_2 on carbons was studied with respect to the basic hydrolysis, thiolysis, aminolysis, reaction with alkyl halides, and photolysis in *tert*-butanol.[17,18] The results showed that the thiolysis and photolysis in *tert*-butanol occurred onto the oxidized intermediates, while only the nonoxidized intermediate was involved in the aminolysis.

Photolytic functionalization of NT has been achieved[19−22] but the effect of the carbon particles on the photolysis of amino acids and the mechanism of their insertion onto the carbon matrix has not been studied. In this work, we have studied the photolysis of phenylalanine, in the presence of multiwalled carbon nanotubes oxidized by different methods and modified after reaction with SO_2. The effect of the carbon particles on the photodecomposition of phenylalanine and its insertion in modified oxidized carbon nanotubes was also studied.

2. EXPERIMENTAL SECTION

2.1. Materials and Methods. All reagents were of analytical grade and were used without further purification. Sulfur dioxide, from White Martins Gases Industriais Ltda., Brazil, was 99.9% pure. The multiwalled carbon nanotubes (NT) were from Nanostructured & Amorphous Materials Inc. (diameter: 20−40 nm, length: 0.5−5 μm, 95% pure). Aqueous solutions were made using bidistilled water treated with $KMnO_4$.

Elemental analyses were obtained in a PerkinElmer-240 analyzer. The sulfur mass content was determined in a LECO SC132 analyzer, and the FTIR spectra were carried out on an ABB Bomem FTLA 2000 spectrometer. Total carbon analysis (TCA) of the photolyzed solutions was performed in a Shimadzu TOC 5000 A.

The XPS spectra were obtained using a VG Microtech ESCA 3000 spectrometer operating with a Mg(K_α) source. The base pressure of the system was in the low 10^{-10} mbar range, and the operating pressure was maintained below 10^{-8} mbar during the measurements. The calibration was carried out with respect to the main C 1s peak at 284.5 eV. The concentration of the elements was calculated using the system database. The deconvolution of the various peaks was obtained using the Spectral Data Processor (SDP) v 4.5.[23]

The HPLC-MS separation was achieved in a LUNA C18 analytical column at 30 °C along with a Thermo Scientific Accela gradient program. The sample volume was 10 μL and the mobile phase A was 0.1% formic acid in water while mobile phase C was methanol. The Thermo Scientific LTQ Orbitrap Discovery mass spectrometer was operated in a positive electrospray ionization (ESI) mode. The source parameters were set as follows: capillary at 360 °C, 35 V, ion spray 5.0 kV.

Solid-state NMR spectra were measured on a Bruker MSL300 spectrometer (7.05 T) using a standard 7 mm MAS probe (Bruker). The measurements were carried at room temperature at the MAS frequency of 4.2 kHz with stability better than ±3 Hz. The high-resolution ^{13}C NMR spectrum was recorded using MAS and high-power ^{1}H decoupling. The RIDE pulse sequence was used for direct detection of ^{13}C with suppression of acoustic ringing effects.[24] Acquisition conditions for the ^{13}C MAS spectrum with direct observation of ^{13}C were as follows: ^{13}C 90° pulse duration = 4.5 μs; recycle delay = 5 s; number of scans = 67 000. The ^{13}C chemical shifts are given relative to tetramethylsilane.

2.2. Oxidation of Carbon Nanotubes with Strong Oxidants.[25] In a 500 mL double wall cylindrical glass vessel, with mechanical stirring, were added 230 mL of sulfuric acid and 10 g of NT. Then, 30 g of $KMnO_4$ were slowly added keeping the temperature below 10 °C. The mixture was cooled to 2 °C and stirred for 30 min, allowing it to warm up to room temperature. Distilled water, 230 mL, was slowly added to the reactor, and the mixture was transferred to a 5 L beaker with stirring and 1.4 L of water was added dropwise, followed by 100 mL of 35% hydrogen peroxide. The dispersion was allowed to decant overnight. The filtered solid was exhaustively washed with water until negative test for sulfate. The oxidized nanotubes were dried under vacuum at 40 °C. The composition of the resulting material was determined from XPS spectrum as C 72.74 at %, O 27.26 at %.

2.3. Oxidation of Carbon Nanotubes with Hydrogen Peroxide.[26,27] The NT sample, 10 g, was added to 100 mL of 35% H_2O_2, and the dispersion was heated to 40 °C for 5 h under constant stirring. The solid was filtered and dried at 100 °C under vacuum. The oxidized NT were kept under nitrogen atmosphere at low temperature. The composition of the resulting material was determined from XPS spectrum as C 70.59 at %, O 29.41 at %.

2.4. Modification of Oxidized Nanotubes by Reaction with SO_2. The sample of oxidized nanotubes, NTO, was dried at 110 °C for 12 h, and after cooling, it was placed in the center of a tubular 316 stainless steel reactor (30 cm height, 2.5 cm diameter) fitted with a temperature controller and heated by an electric oven in a system that has been described in detail previously.[28] The sample was kept under a flow of He until reaching 800 °C. The sample was then allowed to react under a flow of 60 mL·min^{-1} of SO_2 (20% in N_2) and was cooled under He. The residual NTO will be referred as modified oxidized nanotubes, mNTO.

2.5. Photolysis Experiments. Photolyses were carried out on aqueous solutions of the substrate in the absence and presence of NT in a photoreactor at 25 °C with a low-pressure Hg-arc (NK 30/89, Heraeus Noblelight), 15 W, emitting at 254 nm. Unless otherwise

DOI: 10.1021/la503631b
Langmuir 2015, 31, 164−170

Table 1. Type of Sulfur from XPS Spectra of NTO Modified with SO_2

code	oxidation method	reaction time with SO_2,[a] min	sulfur		binding energy, eV	at %
SOmNTO25	strong oxidants	25	S 2p	nonoxi	164.7	0.47
				oxi	169.1	0.08
				total		0.55
SOmNTO48	strong oxidants	48	S 2p	nonoxi	163.5	0.27
				oxi	167.8	0.04
				total		0.31
SOmNTO120	strong oxidants	120	S 2p	nonoxi	164.3	5.91
				oxi		
				total		5.91
H_2O_2mNTO120	H_2O_2	120	S 2p		161.9	0.18
				nonoxi	163.9	0.51
				oxi		
				total		0.69

[a]At 800 °C, flow of SO_2 60 mL·min^{-1}.

Table 2. Rate Constants Ratios of the Photolyses of Aqueous Solutions of Phe in the Presence of NT at 25 °C

substrate	NTO code[a]	S,[b] at %	sulfate,[c] mg/L	10^4slope,[d]	$10^2k^*/k_o^*$[e]
phenylalanine[f]	without NTO			80.7 ± 1.8	100.0
	NTO, without modification			24.6 ± 6.1	30.5
	NT[i]			37.7 ± 4.4	46.8
	MPG[g]			22.3 ± 1.2	27.7
	SOmNTO25	0.55	3.79	47.3 ± 4.4	58.6
	SOmNTO48	0.30	0.96	31.7 ± 9.0	39.3
	SOmNTO120	5.91	1.67	39.0 ± 4.6	48.3
	H_2O_2mNTO120	0.69	1.56	26.7 ± 2.9	33.1

[a]See definition of code in Table 1; 20 mg of NTO in 250 mL photolyzed for 120 min. [b]Sulfur content in NTO from XPS spectra. [c]Sulfate concentration at the end of the photolysis. [d]Slope $p^* = \Delta A/\Delta t$. [e]$p^*/p_o^* = k^*/k_o^*$. [f]Phenylalanine, 0.650 mM, followed at 220 nm. [g]NT, pristine carbon nanotubes; MPG, graphite microparticles. After reaction with O_3 for 180 min at 25 °C.

indicated, the photolyses were carried out in distilled water and under air atmosphere. For the photolysis, NTO were initially dispersed in 50 mL of the amino acid solution and treated with ultrasound for 10 min. The dispersion was added to 200 mL of the substrate solution and placed in the photoreactor previously thermostated at 25 °C. In the presence of NT, samples were taken out with a 5.0 mL syringe, filtered through 0.45 μm nylon filters, and the absorbance measured. All samples were eventually kept in sealed Eppendorf tubes. The final dispersion was allowed to stand for 12 h and was decanted. The solid was dried at 70 °C for 12 h. In the absence of NT, the absorbance of the solution was read continuously in a UV spectrophotometer Hitachi, U3000, using a peristaltic pump to push the solution from the photoreactor into an optical flow cell.

Initial rates were obtained from the plot of ΔA versus Δt, both in the presence of NT ($\Delta A/\Delta t = p^*$), and in their absence ($\Delta A/\Delta t = p_o^*$). The ratio p^*/p_o^* gives the ratio k^*/k_o^* of rate constants of the photolysis in the presence and in the absence of nanotubes, respectively.

2.6. Adsorption of Phenylalanine by NT. In order to verify if the observed results were not simply due to an adsorption-desorption equilibrium, the process was studied for Phe. A dispersion of 20.8 mg of NT in 50 mL of a 0.63 mM Phe solution was sonicated for 10 min. The dispersion was diluted by addition of 150 mL of the solution of Phe in a thermostated vessel at 25 °C, with magnetic stirring and in the dark. Samples of the dispersion (3 mL), were centrifuged and the absorbance of the supernatant measured at 210 nm and compared to the corresponding absorbance of the Phe solution. No adsorption of phenylalanine on NT was observed.

3. RESULTS AND DISCUSSION

The multiwalled carbon nanotubes (NT) used for the photolysis of phenylalanine (Phe) were oxidized by two

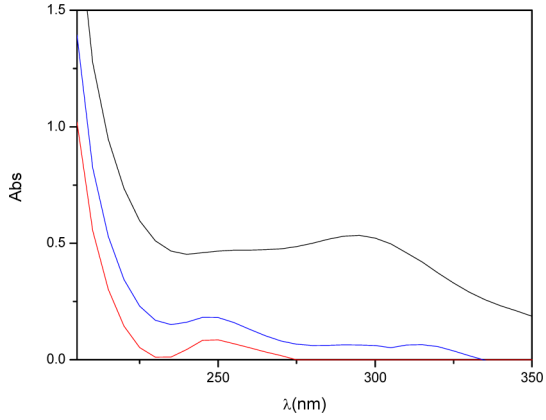

Figure 2. UV spectrum of aqueous solution of phenylalanine, 0.650 mM (red); after photolysis at 254 nm for 90 min, 25 °C (black); in the presence of oxidized carbon nanotubes SOmNTO120 (blue).

Table 3. HPLC/MS Analysis of the Products of the Photolysis of Phenylalanine[a]

	without	NTO	with	NTO[b]
retention time, min	3.45	4.87	3.45	4.87
$[M + H]^+$	182[c]	166[d]	182[c]	166[d]
reaction time, min	%		%	
0	0.00	100.0		100.0
40	18.5	81.5	9.6	90.4

[a]Photolysis at 254 nm, 250 mL, 0.650 mM. [b]20.0 mg, SOmNTO120, see code in Table 1. [c]Tyrosine. [d]Phenylalanine.

DOI: 10.1021/la503631b
Langmuir 2015, 31, 164−170

Table 4. Binding Energies and Composition, As Determined from XPS spectra, of Nanotubes SOmNTO120 after Photolysis in the Presence of Phe[a]

sample		SOmNTO120 initial		after photolysis with Phe[b]		calcd[c]
element		eV (weight %)	at %	eV (weight %)	at %	at %
S 2p	nonoxi			164.38 (53.8)	1.99	
	nonoxi	165.25 (100)	5.91	165.61 (28.0)	1.04	
	oxi			168.25 (18.2)	0.67	
	total		5.91		3.70	3.64
C 1s		285.00 (40.92)	35.56	285.00 (74.4)	68.60	
				285.75 (5.2)	4.79	
		286.33 (59.08)	51.33	286.33 (9.4)	8.67	
				287.60 (6.2)	5.72	
				290.90 (4.8)	4.43	
	total		86.89		92.20	92.31
O 1s				532.03 (49.4)	1.93	
				533.40 (50.6)	1.97	
		535.25 (100)				
	total		7.21		3.90	3.90
N 1s				400.18	0.20	0.20

[a]Spectrum calibrated by reference to C 1s (285.0 eV). [b]Photolysis in air-saturated solution at 254 nm, 25 °C, for 120 min. [c]From the reaction 1: $(CO_2)C(S)\rightarrow C(S)+CO_2$; reaction 2: $C(S)\rightarrow C+S$; reaction 3: $C(S)+H_2NCH(C_7)COOH\rightarrow C(SH)HNCH(C_7)COOH$; reaction 4: $C(SH)HNCH(C_7)COOH\rightarrow C(SH)HNCH_2(C_7)+CO_2$

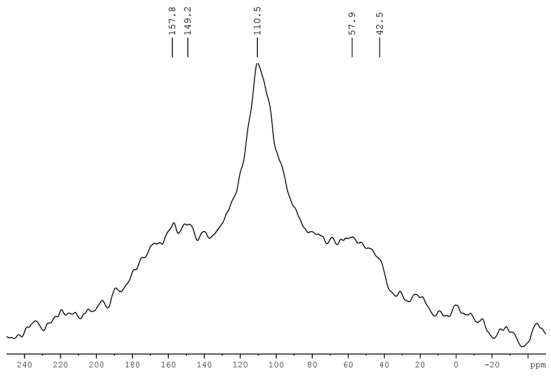

Figure 3. ^{13}C RIDE[24] SSNMR spectrum of modified NT SOmNTO120 upon 120 min of photolysis of Phe in air-saturated solution at 254 nm.

different methods and modified by reaction with SO_2 under different conditions.

3.1. Reaction of Oxidized Carbon Nanotubes NTO with SO_2. It has been found that the reactivity of SO_2 toward graphite and activated carbon,[12,13] as well as NT[9,10] increased by oxidation. Therefore, oxidized carbon nanotubes, NTO, were allowed to react with SO_2 at 800 °C at different times. The results, shown in Table 1, indicate that for NT oxidized with strong oxidants, the oxidized sulfur content decreased with increasing reaction time with SO_2, until disappearance after 120 min. This result is similar for the sample oxidized with H_2O_2. In this particular case, the signal at 161.9 eV can be assigned to elemental sulfur (S 2p3/2, 161.2 eV, S_x, x = 8, 4).[29]

The absence of oxidized intermediates in some cases might be consequence of the high temperature used in the modification. A plausible explanation is the well-known fact that, the concentration of intermediates decreases as the rate-determining step of formation of CO_2 (Figure 1) becomes faster (a reduction in the activation energy for the r.d.s. reduces the depth of the energy well for the formed intermediate, thus destabilizing it).[30]

NT oxidized with H_2O_2, after 2 h of reaction with SO_2 at 650 and 800 °C, showed a drastic decrease of oxygen content (29 to 12 at %), as well as carbon NT oxidized with strong acids (27 to 27 at %). The XPS spectrum suggests[31] that the SO_2 insertion occurred with elimination of CO_2 and oxygen.

3.2. Photolyses of Phenylalanine in the Presence of NTO. Photolyses at 254 nm of aqueous solutions of Phe were carried out in the presence of a constant amount of differently modified NTO, and the relative initial rates obtained after ca. 40 min (Table 2). The presence of NT decreases the relative initial rates k^*/k_o^*, and consequently, the rate of photolytic decay k^* of Phe. A progressive increase of mass of pristine NT led to an exponential decrease of the relative initial rates k^*/k_o^*. Unmodified NTO produced the largest decrease of rate ratios. Sulfate was also detected as product when using modified NTO.

Aqueous solution of Phe showed a UV spectra (Figure 2) with a maximum at 250 nm (literature value λ_{max} = 252 nm, ε = 154 $mol\cdot dm^{-3}\cdot cm^{-1}$).[32] After 90 min of photolysis a new maximum appeared at 295 nm, that can be attributed to tyrosine (Tyr) due to phenolic hydrogen deprotonation in basic media (295 nm, ε = 1000 $mol\cdot dm^{-3}\cdot cm^{-1}$).[33] The substantial decrease of the band of Tyr in the presence of NTO, occurred with an associated decrease of the initial rate ratio (Table 2). The extent of this decrease also depends on the difference of absorbance of the UV spectra of the substrate and the degradation products of the photolysis.

HPLC/MS analysis of the products of the photolysis of Phe was consistent with these findings (Table 3). In the absence of NTO two peaks with retention times 3.45 and 4.87 min, respectively, were observed, corresponding to 18.5% Tyr and 81.5% Phe. Photolysis in the presence of NTO produced the same products, but with 9.6% and 90.4% yields, respectively. Therefore, the presence of NTO inhibited drastically (ca. 50%) the formation of Tyr.

The presence of O_2 has only a minor effect on the photolytic decay of Phe, which is in contrast with the behavior of Tyr,[34−37] for which O_2 largely enhances its photoreactivity. This difference is attributed to the higher quantum yield for the

DOI: 10.1021/la503631b
Langmuir 2015, 31, 164−170

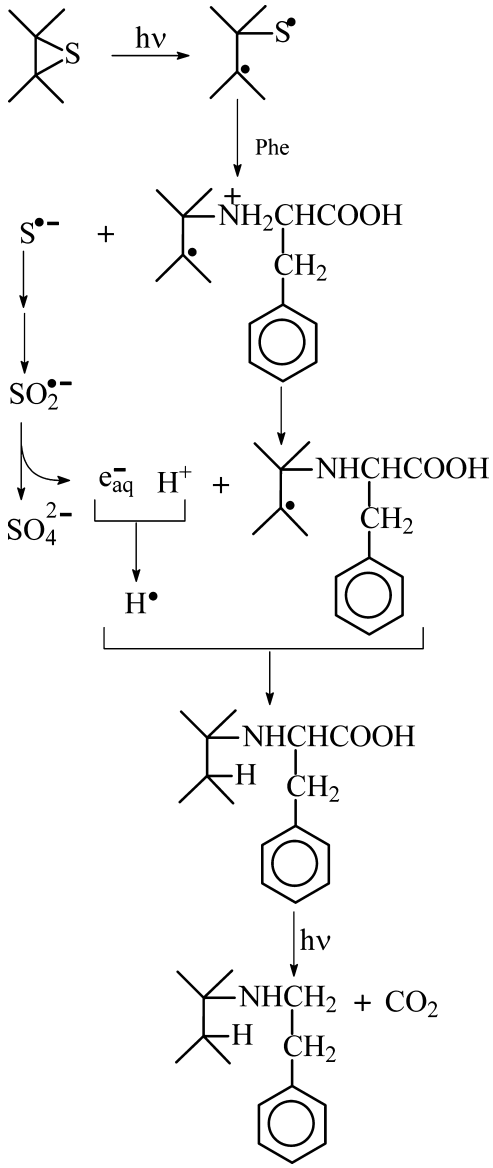

Figure 4. Mechanism of photoinsertion of Phe onto oxidized carbon NT modified with SO_2 at 800 °C.

triplet of Tyr relative to Phe ($\phi_{T,\ Tyr}$ = 0.50, $\phi_{T,\ Phe}$ = 0.40) both determined upon excitation at 266 nm.[36] In the absence of O_2, only stereoisomeric phenylalanyl-bicyclohexenols were observed, generated from the singlet excited state. The amino group was retained, and a molecule of water incorporated. In the presence of O_2 the triplet state was readily quenched[38] and different ring-hydroxylated tyrosines (o, m, p) produced.[39,40] These products can be explained through photoionization of Phe to form the corresponding radical cation,[34] that reacts with water to produce hydrocyclohexadienyl radicals, which further react with O_2 to yield the corresponding hydroxylated tyrosines.[35]

3.3. Photoinsertion of Phenylalanine onto Modified NTO. The photolysis of Phe did not produce CO_2 (less than 1 mg·L^{-1}), but all modified NTO contributed to a reduction of the organic carbon to different extents. The photoinsertion of the amino acid onto oxidized NT modified upon reaction with SO_2 should lead to a decrease of organic carbon in solution, without generation of inorganic carbon (released as CO_2). Therefore, the kinetics of the insertion was studied using total carbon analysis and the first-order rate constant for the decrease of TCA during the Phe photoinsertion on nanotubes SOmNTO120 in air-saturated solution at 25 °C in the presence of 20 mg of SOmNTO120 (Table 1) was k_{in} = 30 ± 6 min^{-1} (r = 0.865). No insertion was detected for the photolysis of Phe in Ar-saturated water: the change of TCA was within the standard deviation.

The reactivity of the intermediates of the reduction of SO_2 on a carbon matrix is selective:[17,18] the thermal reaction of aminolysis took place only on the nonoxidized episulfide intermediate, while photolytic alcoholysis took place on the oxidized intermediate.[18] Photolytic aminolysis has not been studied yet. The XPS spectrum of the nanotubes SOmNTO120 (see Table 1), that contain only nonoxidized intermediate, after photolysis of Phe, is shown in Table 4. The concentration of the nonoxidized intermediate decreased from 5.91 to 3.70 at % of sulfur. The so-released sulfur underwent oxidation to SO_4^{2-} under the experimental conditions. The production of SO_4^{2-} in the final solution upon photolysis of amino acids in the presence of modified NTO was reported in Table 2. The XPS spectrum also shows the presence of nitrogen (0.20 at %) indicating the insertion of the amino acid. The final composition was calculated through the atom inventory technique[31] using the reactions shown in the footnotes of Table 4. Although the method is not capable of distinguishing between Phe and tyrosine, we consider only the insertion of Phe since, according to the HPLC results (Table 3) the concentration of Tyr was very low and the reactivity of the amino group should be very similar for both compounds.

Reaction 1 used to calculate the final XPS spectrum of Table 4 indicates a loss of CO_2 from the carbon matrix according to the mechanism of the primary reaction (Figure 1) where the formation of the episulfide nonoxidized intermediate occurs along with the generation of an oxidized moiety C(CO_2) that produces CO_2 in a further step. The insertion of Phe (reaction 3) extrudes a sulfur species (reaction 2) that is followed by decarboxilation of the inserted species (reaction 4). Both decarboxilation reactions take place at different steps but their extent must be low, as indicated by the low levels of inorganic carbon observed from the TCA.

The ^{13}C SSNMR spectrum of modified NTO after photolysis in the presence of Phe (Figure 3) is compatible with the insertion, providing additional evidence for the reaction.

The reactions of insertion of Phe used to calculate the XPS spectrum suggest the mechanism shown in Figure 4. Modified NTO SOmNTO120 contains only episulfide intermediate, and it is reasonable to assume that the excited state generated upon light absorption, decays in energy by C—S bond homolysis that demands ca. 33 kcal·mol^{-1} to produce the triplet biradical.[41] The sulfur species may extrude upon the insertion of Phe as a sulfide radical anion ($^{\bullet}S^{-}$) that reacts with O_2 to form sulfur dioxide radical anion $SO_2^{\bullet-}$ and subsequently generates SO_4^{2-} by mild oxidation, releasing one solvated electron.[18,42,43]

The presence of nanotubes might decrease the absorption of UV light by Phe preventing its photoionization to form the radical cation, precursor of the hydrocyclohexadienyl radicals which yield the corresponding hydroxylated tyrosines (see above). At the same time excitation of carbon matrix by UV absorption will favor the excited state of the episulfide intermediate to produce C—S homolysis postulated in the mechanism of Figure 4. Further studies are needed regarding the photolysis of carbon nanotubes.

DOI: 10.1021/la503631b
Langmuir 2015, 31, 164−170

The formation of SO_4^{2-} was observed in all the photolysis in the presence of modified NTO (Table 2). Solvated electrons (e^-_{aq}) are also produced in the phototransformation of Phe to Tyr in the presence of O_2. These e^-_{aq} can be captured by H^+ present in the medium or transferred from the amino group or the carboxyl group of the inserted amino acid species. The resulting H● radical would cover the empty radical position left by the sulfide radical anion.

The reaction of intramolecular electron transfer of the Phe radical cation with the carboxylate group is followed by the decarboxylation forming an amino-substituted radical.[44] This radical can be oxidized by oxygen to yield an aldehyde or add a $H^•$ radical from $HO_2^•$ generated in the oxidation of the hydrocyclohexadienyl radicals. However, under the photolytic conditions used in the insertion reaction in the presence of modified NTO, the O_2 concentration is low and the decarboxylation reaction should occur with low yield.

4. CONCLUSIONS

The ratio of the initial rates of photolysis at 254 nm of phenylalanine (Phe), decreases in the presence of carbon nanotubes. The mass of nanotubes produces an exponential attenuation of the photolytic decomposition. The photolytic decay of Phe in air-saturated solution takes place with formation of tyrosine (Tyr), that is inhibited in the presence of NTO.

Total carbon analyses (TCA), ^{13}C-SSNMR, and XPS spectra showed the photofunctionalization of NTO, modified by SO_2, by insertion of Phe onto the nonoxidized episulfide intermediate. The insertion on the matrix may occur along with the extrusion of a sulfide radical anion ($^•S^-$) which undergo subsequent oxidation to SO_4^{2-}.

AUTHOR INFORMATION

Corresponding Author

* Tel: 55 48 3282 1078. E-mail: eduardo.humeres@ufsc.br.

Notes

The authors declare no competing financial interest.

ACKNOWLEDGMENTS

We thank the Brazilian Government Agency *Coordenação de Aperfeiçoamento de Pessoal de Nível Superior* (CAPES), Projeto CAPES/DGU 219/2010, and the Spanish *Ministerio de Educación, Cultura y Deporte*, DGU, Project PHB2009-0057-PC, for financial support.

REFERENCES

(1) Li, J.; Vergne, M. J.; Mowles, E. D.; Zhong, W.-H.; Hercules, D. M.; Lukehart, C. M. Surface functionalization and characterization of graphitic carbon nanofibers (GCNFs). *Carbon* **2005**, *43*, 2883−2893.

(2) Dongil, A. B.; Bachiller-Baeza, B.; Guerrero-Ruiz, A.; Rodriguez-Ramos, I.; Martinez-Alonso, A.; Tascon, J. M. D. Surface chemical modifications induced on high surface area graphite and carbon nanofibers using different oxidation and functionalization treatments. *J. Colloid Interface Sci.* **2011**, *355*, 179−189.

(3) Barroso-Bujans. Degree of functionalization of carbon nanofibers with benzenesulfonic groups in an acid medium. *Carbon* **2007**, *45*, 1669−1678.

(4) Schaetz, A.; Zeltner, M.; Stark, W. J. Carbon Modifications and Surfaces for Catalytic Organic Transformations. *ACS Catal.* **2012**, *2*, 1267−1284.

(5) Li, J. In *Carbon Materials for Catalysis*; P. Serp, J. L. Figueiredo, Eds.; Wiley: New Jersey, 2009; pp 507−533.

(6) Ajayan, P. M. Nanotubes from Carbon. *Chem. Rev.* **1999**, *99*, 1787−1799.

(7) Bethune, D. S.; Kiang, C. H.; Devries, M.; Gorman, S. G.; Savoy, R.; Vazquez, J.; Beyers, R. Cobalt-catalysed growth of carbon nanotubes with single-atomic-layer walls. *Nature* **1993**, *363*, 605−607.

(8) Prato, M.; Kostarelos, K.; Bianco, A. Functionalized Carbon Nanotubes in Drug Design and Discovery. *Acc. Chem. Res.* **2008**, *41*, 60−68.

(9) Tasis, D.; Tagmatarchis, N.; Bianco, A.; Prato, M. Chemistry of Carbon Nanotubes. *Chem. Rev.* **2006**, *106*, 1105−1136.

(10) Liu, J.; Rinzler, A. G.; Dai, H. J.; Hafner, H.; Bradley, R. K.; Boul, P.; Lu, J.; Iverson, A.; Shelimov, T. K.; Huffman, C. B.; Rodriguez-Macias, F.; Shon, Y. S.; Lee, T. R.; Colbert, D. T.; Smalley, R. E. Fullerene Pipe. *Science* **1998**, *280*, 1253−1256.

(11) Bonifazi, D.; Nacci, C.; Marega, R.; Campidelli, S.; Ceballos, G.; Modesti, S.; Meneghetti, M.; Prato, M. Microscopic and Spectroscopic Characterization of Paintbrush-like Single-walled Carbon Nanotubes. *Nano Lett.* **2006**, *6*, 1408−1414.

(12) Humeres, E.; Moreira, R. F. P. M.; Peruch, M. G. B. Reduction of SO_2 on Different Carbons. *Carbon* **2002**, *40*, 751−760.

(13) Humeres, E.; Peruch, M. G. B.; Moreira, R. F. P. M.; Schreiner, W. Reactive Intermediates of the Reduction of SO_2 on Activated Carbon. *J. Phys. Org. Chem.* . **2003**, *16*, 824−830.

(14) Pliego, J. R.; Resende, S. M.; Humeres, E. Chemisorption of SO_2 on Graphite Surface: A Theoretical ab Initio and Ideal lattice Gas Model Study. *Chem. Phys.* **2005**, *314*, 127−133.

(15) Humeres, E.; Peruch, M. G. B.; Moreira, R. F. P. M.; Schreiner, W. Reduction of Sulfur Dioxide on Carbons Catalyzed by Salts. *Int. J. Mol. Sci.* **2005**, *6*, 130−142.

(16) Humeres, E.; Moreira, R. F. P. M. Kinetics and Mechanisms in Flow Systems: Reduction of SO_2 on Carbons. *J. Phys. Org. Chem.* **2012**, *25*, 1012−1026.

(17) Humeres, E.; Castro, K. M.; Smaniotto, A.; Lopes, C. N.; Debacher, N. A.; Moreira, R. F. P. M.; Schreiner, W. H.; Aliev, A. E. Reactivity of the Intermediates of the Reduction of SO_2. Functionalization of Graphite, Graphite Oxide and Graphene Oxide. *J. Phys. Org. Chem.* **2014**, *27*, 344−351.

(18) Humeres, E.; Castro, K. M.; Peruch, M. G. B.; Moreira, R. F. P. M.; Schreiner, W. H. E.; Canle, M.; Santaballa, J. A.; Fernandez, I. Reactivity of the Thermally Stable Intermediates of the Reduction of SO_2 on Carbons and Mechanisms of Insertion of Organic Moieties in the Carbon Matrix. *J. Phys. Chem. C* **2008**, *112*, 581−589.

(19) Ahmad, M. N.; Nadeem, M.; Ma, Y.; Yang, W. Photochemical Modification of Single-Walled Carbon Nanotubes Using HPHMP Photoinitiator for Enhanced Organic Solvent Dispersion. *J. Mater. Sci.* **2010**, *45*, 5591−5597.

(20) Nakamura, T.; Ishihara, M.; Ohana, T.; Tanaka, A.; Koga, Y. Sidewall Modification of Single-Walled Carbon Nanotubes Using Photolysis of Perfluoroazooctane. *Diamond Relat. Mater.* **2004**, *13*, 1971−1974.

(21) Nakamura, T.; Ishihara, M.; Ohana, T.; Ohgami, A.; Kosaka, T. Photochemical Modification of Single-Walled Carbon Nanotubes with Thiol and Amino Functionalities and Their Metal Nanoparticle Attachment. *New Diamond Front. Carbon Technol.* **2007**, *17*, 309−320.

(22) Nakamura, T.; Ishihara, M.; Ohana, T.; Hasegawa, Y.; Koga, Y. Photochemical Modification of Single-Walled Carbon Nanotubes With Amino Functionalities and Their Metal Nanoparticles Attachment. *Diamond Relat. Mater.* **2008**, *17*, 559−562.

(23) XPS International, 754 Leona Lane, Mountain View, CA, USA.

(24) Belton, P. S.; Cox, I. J.; Harris, R. K. Experimental sulphur-33 nuclear magnetic resonance spectroscopy. *J.C.S. Faraday Trans.* **1985**, *81*, 63−75.

(25) Bissessur, R.; Scully, S. F. Intercalation of Solid Polymer Electrolytes Into Graphite Oxide. *Solid State Ionics* **2007**, *178*, 877−882.

(26) Lopes, C. N. Síntese e Caracterização do Compósito de Poliestireno/Grafite Produzido Através do Processo de Polimerização em Suspensão, Ph. D. Thesis; Universidade Federal de Santa Catarina: Brazil, 2007.

DOI: 10.1021/la503631b
Langmuir 2015, 31, 164−170

(27) Paggi, R. A. Sinterização Seletiva a Laser de Compósitos com Gradiente Funcional entre Poliamida 12 e Nanotubos de Carbono Aplicáveis no Setor Aeroespacial, M.Sc. Dissertation; Universidade Federal de Santa Catarina: Brazil, 2008.
(28) Humeres, E.; Moreira, R. F. P. M.; Peruch, M. G. B Reduction of SO_2 on Different Carbons. *Carbon* **2002**, *40*, 751−760.
(29) NIST X-ray Photoelectron Spectroscopy Database 20, Version 4.1.
(30) Moore, J.W.; Pearson, R.G. *Kinetics and Mechanism*; Wiley: New York, 1981; Ch 8.
(31) Humeres, E.; Castro, K. M.; Moreira, R. F. P. M.; Schreiner, W. H.; Aliev, A. E.; Canle, M.; Santaballa, J. A.; Fernandez, I. The use of XPS spectra for the study of reaction mechanisms: the atom inventory method. *J. Phys. Org. Chem.* **2008**, *21*, 1035−1042.
(32) Mihalyi, E. Numerical Values of The Absorbances of the Aromatic Amino Acids in Acid, Neutral, and Alkaline Solutions. *J. Chem. Eng.* **1968**, *13*, 179−182.
(33) Wetlaufer, D.B. Ultraviolet spectra of Proteins and Amino Acids. *Adv. Protein Chem.* **1963**, *17*, 303−390.
(34) Canle, M. L.; Santaballa, J. A.; Steenken, S. Photo- and Radiation-Chemical Generation and Thermodynamic Properties of the Aminium and Aminyl Radicals Derived from *N*-Phenylglycine and (*N*-Chloro,*N*-phenyl)glycine in Aqueous Solution: Evidence for a New Photoionization Mechanism for Aromatic Amines. *Chem.—Eur. J.* **1999**, *5*, 1192−1201.
(35) Jin, F.; Leitich, J.; Von Sonntag, C. Photolysis (λ = 254 nm) of Phenylalanine in Aqueous Solution. *J. Photochem. Photobiol. A: Chem.* **1995**, *85*, 101−109.
(36) Chin, K.; Trevithick-Sutton, C. C.; McCallum, J.; Jockusch, S.; Turro, N. J.; Scaiano, J. C.; Foote, C. S.; Garcia-Garibay, M. A. Quantitative Determination of Singlet Oxygen Generated by Excited State Aromatic Amino Acids, Proteins, and Immunoglobulins. *J. Am. Chem. Soc.* **2008**, *130*, 6912−6913.
(37) Jin, F.; Leitich, J.; von Sonntag, C. The Photolysis (λ = 254 nm) of Tyrosine in Aqueous Solutions in the absence and Presence of Oxygen. The Reaction of Tyrosine with Singlet Oxygen. *J. Photochem. Photobiol. A: Chem.* **1995**, *92*, 147−153.
(38) Bent, D. V.; Hayon, E. Excited State Chemistry of Aromatic Amino Acids And Related Peptides. II. Phenylalanine. *J. Am. Chem. Soc.* **1975**, *97*, 2606−2612.
(39) Kenyon, D. H.; Blois, M. S. π-Electron Photochemistry of DL-Phenylalanine in Oxygen Saturated And Oxygen Free Solutions. *Photochem. Photobiol.* **1965**, *4*, 335−349.
(40) Ishimitsu, S.; Fujimoto, S.; Ohara, A. Chemical Modification by 2, 4, 6-Trinitrobenzenesulfonic Acid (TNBS) of an Essential Amino Group in 3-Ketovalidoxylamine A C-N Lyase. *Chem. Pharm. Bull.* **1990**, *38*, 1417−1418.
(41) Zoller, U.; Pastersky, E. I.; Stlenak, S.; Apeloig, Y. Polycyclic arene episulfides. Attempted synthesis, molecular orbital calculations and comparison with arene oxides. *Tetrahedron.* **1998**, *54*, 14283−14300.
(42) Das, T. N.; Huie, R. E.; Neta, P.; Padmaya, S. Reduction Potential of the Sulfhydryl Radical: Pulse Radiolysis and Laser Flash Photolysis Studies of the Formation and Reactions of SH and $HSSH^{\bullet-}$ in Aqueous Solutions. *J. Phys. Chem. A* **1999**, *103*, 5221−5226.
(43) Barbieri, W.; Bernardi, L.; Coda, S.; Vigevani, A. Synthesis and reactions of 1,2-benzoxathian-4-one 2-oxides. *Tetrahedron Lett.* **1971**, *52*, 4913−4914.
(44) Wang, D.; H. Schuchmann, P.; von Sonntag, C. Phenylalanine: Its OH and $SO_4^{\bullet-}$ Induced Oxidation and Decarboxylation. A Pulse Radiolysis and Product Analysis Study. *Z. Naturforsch. B* **1993**, *48*, 761−770.

DOI: 10.1021/la503631b
Langmuir 2015, 31, 164−170